Earth and Planetary Science Letters, 73 (1985) 285–298
Elsevier Science Publishers B.V., Amsterdam – Printed in The Netherlands

[6]

Rare earth elements in foraminifera tests

M.R. Palmer *

Department of Earth Sciences, The University of Leeds, Leeds LS2 9JT (U.K.)

Received August 31, 1984
Revised version received January 11, 1985

The concentrations of nine rare earth elements (REE) La, Ce, Nd, Sm, Eu, Gd, Dy, Er and Yb, have been determined in mixed species assemblages of foraminifera tests taken from Atlantic Ocean sediment core tops. Reductive cleaning techniques have revealed that REE are present in three phases in foraminifera tests collected from sea floor sediments; REE included in the foraminiferal calcite matrix (termed lattice REE), REE associated with an authigenic FeMn-rich phase adsorbed onto the surface of the test following the death of the organism (termed coating REE) and REE associated with alumino-silicate detritus (termed detrital REE) which commonly infills the test chambers after burial in the sediment. The concentrations of REE in the nondetrital (lattice plus coating) and lattice phases have been measured in this study. Approximately 90% of the REE measured in the non-detrital phase reside in the coating phase, the remainder being present in the lattice phase. These data have been used to investigate the relationship between the distribution of dissolved REE in the ocean and in the coating and lattice phases. In addition to the REE the concentrations of Mn, Fe, Cu, Al and PO_4 have been measured as an aid to characterisation of the various phases.

1. Introduction

A major goal of marine chemistry has been to determine the physical and chemical history of the oceans. Stable isotope and micropalaeontological studies have revealed much about past ocean climate and circulation conditions [1,2]. Recent studies have also utilised the trace element contents of foraminiferal calcite to deduce the history of deep ocean nutrient concentrations, circulation patterns and oceanic inputs [3–5].

The chemistry of the REE makes them especially suited to such studies. Chemically they are a very coherent group, and their relative abundances can be used as a "fingerprint" to determine their sources in sedimentary deposits and in solution. Subtle differences in chemical behaviour within the group provide additional information. The stability constants of REE complexes vary in an ordered way. Hence partioning of the REE between phases may lead to fractionation of the light REE relative to the heavy REE. Although the REE exist predominantly as 3 + cations in the marine environment, there are important exceptions, namely Ce which can exist as Ce^{4+} and Eu which can exist as Eu^{2+} Thus these two elements may fractionate from the 3 + cations as a function of redox potential [6–8]. The distribution of dissolved heavy REE in the water column is very similar to that of Si [8–11], thus their concentrations in foraminiferal calcite may serve as proxy indicators of oceanic silicate concentrations.

This investigation was undertaken to evaluate the potential of using the REE concentrations in foraminiferal calcite as palaeo-ocean chemistry indicators by determining whether the analytical methods employed allow reproducible results to be obtained which can then be logically explained in terms of the chemical properties of the REE.

* Present address: Department of Geology and Geophysics, Yale University, New Haven, Conn. 06511, U.S.A.

0012-821X/85/$03.30

2. Sample strategy

Within an individual foraminifera species different sized individuals have differing carbon and oxygen isotope ratios [12]. In addition, the distribution of some elements (e.g. Mg), and oxygen and carbon isotopes may not be homogeneous within an individual test [13–15]. There are also considerable inter-species differences in trace element concentrations [3,16]. However, the amount of cleaned foraminiferal calcite required for the REE analyses (at least 5 mg) and the bulk sample size available (3 g) did not allow single species to be analysed. Whilst this inhibits the use of these data in precise geographical studies it will be shown that the approach adopted here has yielded valuable information concerning the controls over the incorporation of REE in foraminiferal calcite which may be used in later, more specific, investigations.

3. Methods

3.1. Sample preparation

Samples were taken from the top 1 cm of carbonate-rich cores from the Atlantic Ocean. Where possible sediment was taken from trigger weight and box cores as these contain the least disturbed sediment tops. The core locations are listed in the Appendix 1.

The raw sediment was disaggregated by soaking overnight in distilled water. The sediment slurry was then sieved through a 170 μm mesh and washed thoroughly to remove sea salts. The non-foraminiferal material was removed from the remaining sediment by hand picking under a binocular microscope. The tests were crushed with a glass rod to break open the chambers and repeatedly ultrasonically cleaned in quartz distilled (QD) H_2O and QD methanol until the supernatant remained clear. The samples were re-examined under a binocular microscope to ensure that all visible adhering detritus had been removed.

The FeMn-rich coating is chemically bound to the foraminiferal calcite and cannot be removed by physical cleaning methods alone. Boyle developed a reductive cleaning method to remove such coatings. The technique consists of physically cleaning the tests (as described above) followed by soaking the crushed $CaCO_3$ in a warm reducing solution [3].

Following the soaking stage above, the reducing solution was drained off and the sample ultrasonically agitated in QD H_2O and QD methanol three times each, for intervals of one minute, to remove any remaining traces of the solution. The sample was transferred to a teflon bottle containing 20 ml of QD H_2O and dissolved by bubbling filtered CO_2 gas through the water for six hours. The bottle was immersed in an ice bath to increase the solubility of CO_2. The sample was then centri-

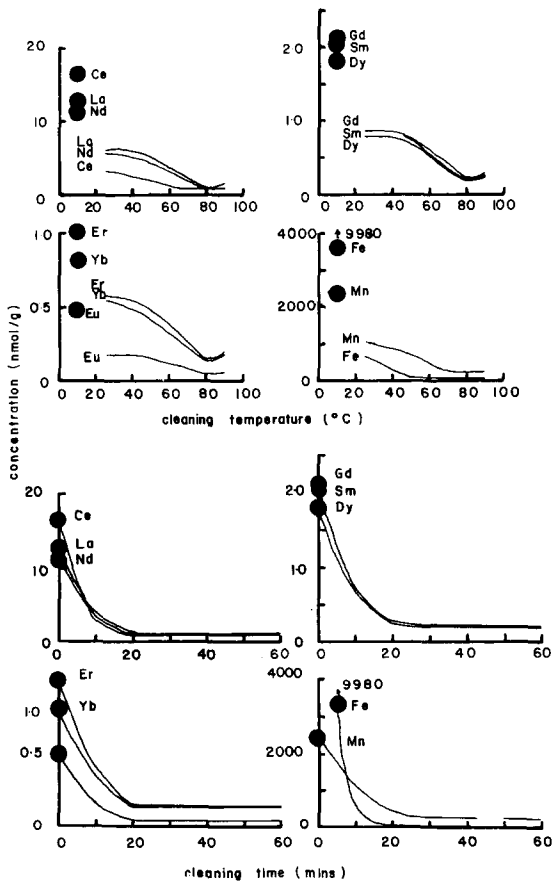

Fig. 1. The effect of variations in cleaning times and temperatures on foraminiferal REE, Fe and Mn concentrations. The circles indicate the original concentrations in the non-detrital phase prior to cleaning.

TABLE 1

Non-detrital concentrations

Sample	Ca	Fe	Mn	Cu	PO_4	Al	La	Ce	Nd	Sm	Eu	Gd	Dy	Er	Yb
1 [a]	39.87	230	35	4.7	920	1230	1.15	1.20	1.38	0.312	0.071	0.300	0.260	0.135	0.112
2	39.49	4860	477	9.4	860	250	2.95	6.61	3.28	0.716	0.179	0.671	0.681	0.361	0.276
3	39.53	3890	355	11.8	1980	2620	2.18	4.38	2.13	0.448	0.110	0.492	0.392	0.210	0.171
4	39.78	2190	92	–	1330	480	2.41	2.22	2.20	0.451	0.110	0.613?	0.479	0.297	0.265
5	39.83	250	61	4.1	500	150	1.96	1.07	1.81	0.377	0.089	0.390	0.369	0.209	0.167
6 [a]	39.65	1530	230	–	660	770	1.08	1.37	1.04	0.199	0.049	0.198	0.178	0.120	0.088
7	39.68	1870	320	10.0	1040	210	1.91	1.72	1.74	0.364	0.088	0.373	0.324	0.174	0.140
8	39.82	740	200	90.5?	700	380	2.20	3.24	2.05	0.417	0.096	0.420	0.348	0.212	0.163
9	39.78	1300	170	7.0	580	560	0.92	0.92	0.73	0.142	0.033	0.148	0.129	0.073	0.057
10 [a]	39.78	2000	350	10.0	840	2370	1.27	1.66	1.05	0.206	0.048	0.211	0.180	0.101	0.080
11	39.73	1200	140	12.5	620	740	1.17	0.90	0.96	0.196	0.046	0.215	0.199	0.120	0.097
12 [a]	39.69	1710	370	10.2	640	1600	1.85	2.18	1.73	0.383	0.098	0.440	0.363	0.199	0.161
13 [a]	39.73	2230	590	17.9	600	660	2.09	1.43	2.15	0.454	0.107	0.459	0.357	0.237	0.169
14	39.66	1750	280	16.1	2010	700	1.45	1.86	1.38	0.275	0.064	0.284	0.267	0.132	0.092
15	39.72	1990	190	-	890	700	1.81	2.26	1.74	0.359	0.087	0.392	0.339	0.191	0.155
Average	39.72	1820	257	10.3	943	870	1.76	2.20	1.69	0.353	0.085	0.374	0.324	0.185	0.146

Ca as molar %, all other elements are as μmol/mol Ca.

[a] Samples analysed for both non-detrital and lattice concentrations. ?: anomalous data.

TABLE 2

Lattice concentrations

Sample	Fe	Mn	Cu	Al	La	Ce	Nd	Sm	Eu	Gd	Dy	Er	Yb
1 [a]	1.48	8.4	0.15	2.3	0.123	0.0890	0.0930	0.0174	0.0042	0.0217	0.0259	0.0159	0.0146
6 [a]	6.15	26.7	0.93	2.1	0.081	0.0348	0.0629	0.0107	0.0028	0.0184	0.0221	0.0126	0.0134
10 [a]	3.41	7.2	0.27	7.6	0.162	0.0983	0.1170	0.0220	0.0051	0.0271	0.0327	0.0246	0.0231
12 [a]	11.80	16.0	1.12	1.9	0.105	0.0950	0.0911	0.0231	0.0052	0.0217	0.0187	0.0149	0.0146
13 [a]	3.56	30.2	0.40	2.1	0.294	0.1360	0.2510	0.0485	0.0113	0.0632	0.0481	0.0334	0.0292
16	5.33	26.9	0.30	11.1	0.289	0.2730	0.2510	0.0473	0.0125	0.0587	0.0603	0.0448	0.0361?
17	3.01	5.9	0.48	4.2	0.091	0.0715	0.0758	0.0145	0.0035	0.0210?	0.0147	0.0091	0.0084?
18	3.51	6.3	0.30	19.8	0.116	0.0720	0.0994	0.0173	0.0044	0.0192	0.0178	0.0131	0.0149
19	3.17	11.1	0.35	13.1	0.297	0.2350	0.2380	0.0519	0.0119	0.0494	0.0414	0.0296	0.0263
20	9.23	23.0	1.07	13.1	0.177	0.1160	0.1710	0.0367	0.0102	0.0500	0.0455	0.0331	0.0303
21	2.93	4.9	0.25	2.6	0.362	0.1430	0.2820	0.1110?	0.0125	0.0524	0.0472	0.0330	0.0311
22	7.03	10.4	0.60	8.2	0.227	0.1920	0.1860	0.0328	0.0074	0.0388	0.0472	0.0332	0.0058?
23	2.14	13.4	0.73	9.7	0.076	0.0420	0.0653	0.0127	0.0030	0.0130	0.0132	0.0094	0.0085
24	5.04	9.1	0.12	7.1	0.065	0.0452	0.0614	0.0120	0.0027	0.0130	0.0126	0.0090	0.0086
25	3.44	6.3	0.38	9.4	0.334	0.1970	0.2870	0.0480	0.0103	0.0431	0.0452	0.0319	0.0322
26	2.27	4.8	0.45	4.8	3.99?	3.59?	2.16?	0.414?	0.087?	0.389?	0.464?	0.376?	0.497?
27	1.73	15.0	0.54	5.6	0.099	0.0785	0.0800	0.0140	0.0030	0.0131	0.0152	0.0103	0.0102
28	6.63	22.7	0.57	11.2	0.093	0.1120	0.0795	0.0147	0.0033	0.0166	0.0183	0.0126	0.0117
29	2.55	7.6	0.33	4.5	0.174	0.0929	0.1320	0.0256	0.0061	0.0253	0.0241	0.0206	0.0179
30	4.98	11.4	0.49	6.4	0.122	0.0869	0.1360	0.0251	0.0058	0.0299	0.0310	0.0213	0.0195
31	9.32	5.6	0.60	9.3	0.414	0.4560	0.4700	0.0972	0.0226	0.1120	0.0931	0.0736	0.0723
Average	4.70	13.0	0.50	7.4	0.185	0.133	0.162	0.0301	0.0074	0.0361	0.0337	0.0243	0.0230

Concentrations are expressed as μmol/mol Ca.

[a] samples analysed for both non-detrital and lattice concentrations. ?: anomalous data. All PO_4 concentrations are below the detection limit of 10 μmol/mol Ca. All Ca concentrations are equal to 39.92 molar % (within analytical error).

fuged and the solution transferred to a teflon beaker before being evaporated to dryness.

To determine the optimum cleaning temperature five splits of an homogenised sample were cleaned for 30 minutes at 25°C, 50°C, 65°C, 80°C and 90°C. The time required for effective cleaning was determined by cleaning five further splits of the same sample at 80°C for 10, 20, 30, 45 and 60 minutes. The results of these experiments are illustrated in Fig. 1.

On the basis of these results a cleaning regime of 30 minutes at 80°C was routinely employed for removal of the coating phase.

3.2. Sample analysis

Elemental concentrations in the non-detrital phase were determined by dissolving the sample overnight in 0.1 M QD HCl (after ultrasonic cleaning). Concentrations in the lattice phase were determined using the techniques described above.

The REE concentrations were determined by mass spectrometric isotope dilution [17]. Fe, Mn, Cu and Al concentrations were determined by atomic absorption spectrophotometry. PO_4 concentrations were measured spectrophotometrically using a continuous flow autoanalyser. Ca concentrations were determined by titration against EGTA [18].

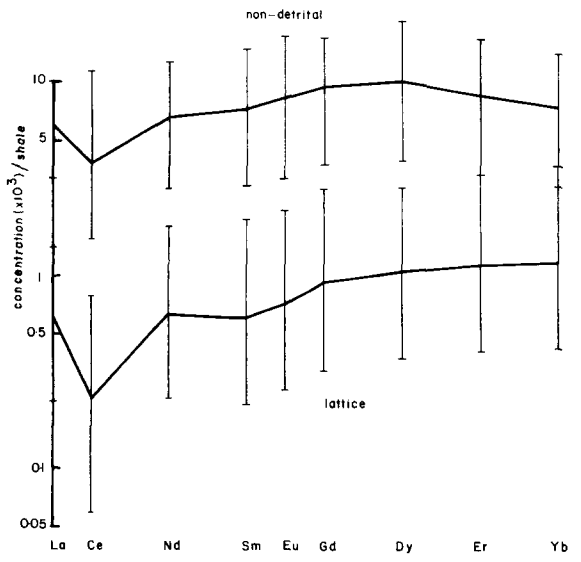

Fig. 2. Average REE patterns of non-detrital and lattice phases. Vertical bars give the range in values.

The results are listed in Tables 1 and 2. The average REE patterns of the non-detrital and lattice phases (normalised to average shale [19]) are illustrated in Fig. 2, together with range in concentrations for each element. The shapes of the non-detrital REE patterns do not vary significantly between different samples (with the exception of Ce). Similarly the shapes of the lattice REE patterns are very similar to one another. The data precision is discussed below.

4. Data evaluation

To assess the analytical reproducibility a further ten splits of the homogenised sample (the same as that used in the cleaning experiments) were taken and the lattice and non-detrital concentrations were determined in five splits each. The results are summarised in Table 3. The precision is excellent for all the elements measured, with the exception of Cu which, as found by Boyle [3], suffers from residual contamination.

The FeMn-rich coating incorporates high concentrations of a wide variety of trace elements [3,20]. This is well illustrated for the REE by the relatively high correlation coefficients between the

TABLE 3

Results of non-detrital and lattice analyses of five splits each of an homogenised sample (see text for details)

Element	Non-detrital		Lattice	
	mean	st. error	mean	st. error
La	1.26	±0.96%	0.124	±5.20%
Ce	1.66	±0.27%	0.105	±1.24%
Nd	1.10	±0.41%	0.106	±0.67%
Sm	0.21	±0.22%	0.019	±2.16%
Eu	0.05	±0.83%	0.004	±1.67%
Gd	0.21	±0.34%	0.022	±1.19%
Dy	0.18	±1.93%	0.024	±2.11%
Er	0.10	±0.89%	0.017	±3.08%
Yb	0.08	±1.70%	0.015	±3.08%
Fe	995	±1.22%	6.4	±1.26%
Mn	240	±3.19%	2.3	±0.93%
Cu	13	±10.7%	0.7	±16.9%
PO_4	11	±4.96%	–	–

Units are μmol/mol Ca.

non-detrital REE and Fe concentrations (see Fig. 3). A measure of the effectiveness of the cleaning technique is given by the absence of any significant correlation between the lattice REE and Fe concentrations (see Fig. 3).

No significant relationship is observed between either non-detrital or lattice REE and Al concentrations, suggesting that detrital contamination is less serious for the REE compared to uranium [21]. However, if it is assumed that all the Al measured is in fact due to residual detrital contamination, and that this detrital material has REE/Al ratios similar to those of shale and deep-sea pelagic clays [6,7,19,22], the percentage of REE derived from this contaminant source can be estimated. The average contribution of detrital REE to the REE measured in the non-detrital phase is calculated to be less than 4% (maximum of 10% for sample V23-41TW). For the lattice phase, detrital REE contamination is less than 0.4%, i.e., within analytical error.

As a comparative check a monospecific sample (V22-219 *G. truncatuloides*) cleaned by Ed Boyle at M.I.T. was analysed for REE at Leeds. The results fall well within the range of values observed in this study (see Table 4). There is also good agreement between the average lattice Al, Cu, Mn and Fe concentrations measured in this study with those of Boyle [3].

The ranges in lattice Al, Cu, Mn and Fe con-

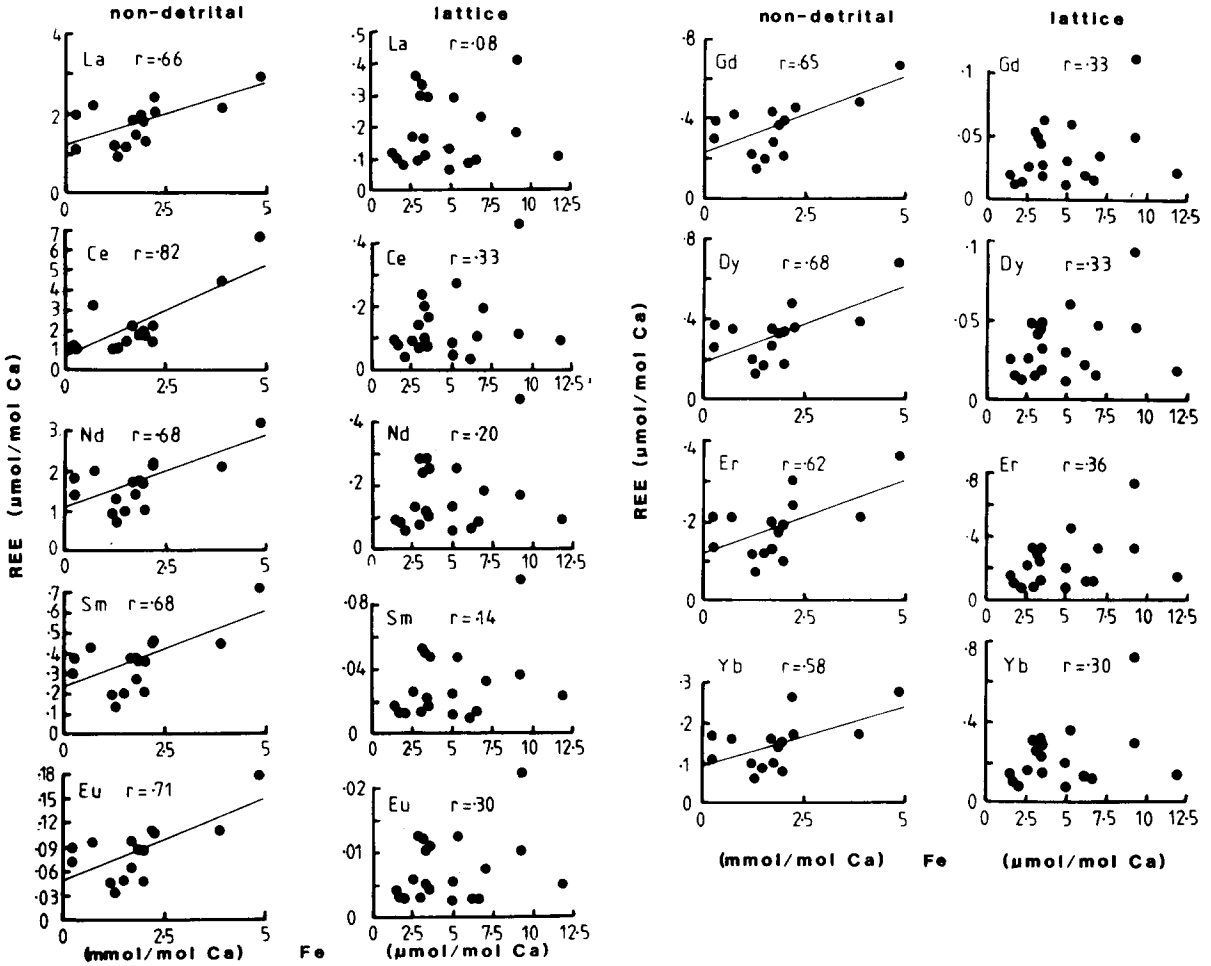

Fig. 3. Relationships between REE and Fe non-detrital and lattice phase concentrations.

TABLE 4

Average and ranges of element/Ca molar ratios from this study and REE in a monospecific sample cleaned by Ed Boyle. Fe, Mn, Cu and Al data from Boyle [3]

Element	Cleaned at Leeds		Cleaned at M.I.T.	
	average	range	conc.	range
La	0.1854	0.4140–0.0646	0.1780	
Ce	0.1332	0.4560–0.0348	0.1390	
Nd	0.1624	0.4700–0.0614	0.1340	
Sm	0.0301	0.0972–0.0107	0.0241	
Eu	0.0074	0.0226–0.0026	0.0054	
Gd	0.0361	0.1120–0.0130	0.0247	
Dy	0.0337	0.0931–0.0126	0.0237	
Er	0.0243	0.0736–0.0090	0.0153	
Yb	0.0230	0.0723–0.0085	0.0138	
Fe	4.70	11.80 –1.48	3.44 [a]	22.1 –0.0
Mn	12.98	30.21 –4.89	12.50 [a]	38.3 –0.0
Cu	0.5	1.12 –0.12	0.45 [a]	7.07–0.03
Al	8.4	19.8 –1.9	13.36 [a]	291.6 –1.3

Units are μmol/mol Ca.
[a] Average.

centrations measured in this study are less than those observed by Boyle [3] despite the close similarity in the average values. This may be because Boyle [3] considers that some of the high Fe, Mn and Al concentrations he observed after cleaning are due to slight residual contamination.

In five cases there was sufficient sample available to permit both lattice and non-detrital REE concentrations to be determined. No clear relationship exists between the REE concentrations in both phases. This indicates that the cleaning technique removes all significant amounts of REE in the non-lattice phases and not just a proportion of the coating.

Because marine phosphatic phases are rich in REE [6,7,23–25] it is important to assess the influence of residual PO_4 contamination on the REE concentrations reported here. The upper limit of Nd concentrations in modern phosphorites and fish debris is approximately 2 μmol/g [6,7,24,25]. Using this Nd/PO_4 ratio and the PO_4 concentrations measured here, a maximum of 2% of the Nd in the lattice phase and 10% in the non-detrital phase are calculated to be associated with residual PO_4. These are upper limits and the probable extent of residual PO_4 contamination is less than half these values.

In all cases the blank levels lay within the precisions quoted above.

All the above evidence indicates that the reductive cleaning procedure is effective in removing all significant amounts of REE present in non-detrital contaminant phases, thus allowing the lattice REE concentrations to be accurately determined.

5. Discussion

5.1. Coating REE

The composition of the coating may be determined by assuming that the amount of Ca associated with the coating is negligible compared with that present in the biogenically precipitated calcite, i.e., the difference between the Ca concentrations in the lattice and non-detrital phases is assumed to be solely due to dilution of the Ca in the non-detrital phase by the coating weight. From the lattice REE/Ca molar ratios and the non-detrital REE and Ca concentrations it is possible to determine the proportions of the non-detrital REE present in the coating and lattice phases (the non-detrital concentrations are corrected for residual detrital contamination in the manner described above). The weight of the coating, and hence its REE concentration is given by:

coating weight = sample weight

$$\times\left[1-\left(\frac{[\mathrm{Ca}]_{\text{non-detrital}}}{[\mathrm{Ca}]_{\text{lattice}}}\right)\right]$$

where [Ca] is the Ca concentration in the relevant phase. The Ca concentrations are the averages in the two phases and the sample weight is the average for the samples analysed for their non-detrital concentrations.

The weight of the coating may also be determined by assuming it consists entirely of Fe_2O_3 and MnO_2 and using the measured non-detrital Fe and Mn concentrations (assuming that the Fe and Mn associated with the lattice phase is negligible). This method yields coating weights that are approximately 25% higher than those calculated from the Ca concentrations.

The average of these two calculations, together

TABLE 5

Concentrations of REE, Fe and Mn in foraminiferal non-detrital, coating and lattice phases, and in other ferromanganese deposits

Phase	La	Ce	Nd	Sm	Eu	Gd	Dy	Er	Yb	Fe	Mn
Average non-detrital	0.0442	0.0551	0.0423	0.0088	0.0021	0.0094	0.0081	0.0046	0.0037	45.5	6.42
Average non-detrital (corrected for detrital contamination)	0.0421	0.0513	0.0406	0.0085	0.0020	0.0091	0.0079	0.0045	0.0035	40.1	6.33
Average lattice	0.00463	0.00333	0.00405	0.00075	0.00018	0.00090	0.00085	0.00060	0.00058	0.118	0.325
% residing in coating	89.0	93.5	90.0	91.1	91.0	90.1	89.3	86.4	83.7	99.7	94.9
Concentration in coating	3.39	4.33	3.30	0.70	0.17	0.75	0.64	0.27	0.26	3610	542
Average Mn nodule [23]	0.73	3.00	0.99	0.23	0.05	0.21	0.19	0.10	0.09	1399	4278
Average micromodule [26]	2.98	9.87	3.58	1.02	0.21	–	–	–	0.20	1487	5771
Average shallow water Mn nodule [6]	1.76	5.55	1.66	0.28	0.06	–	–	–	0.14	–	–
Ferromanganese crust [27]	0.87	0.88	0.68	0.14	0.03	0.16	0.16	0.10	0.09	2884	2403

Units are μmol/g.

with the average REE, Mn and Fe concentrations in other types of FeMn-rich deposits, are shown in Table 5. Although the concentrations in the coating phase are at most only precise to 25%, the interelement relationships and the REE pattern shapes are not affected.

The source of the REE in the coating phase has not yet been unequivocally determined. It is likely that foraminifera tests scavenge some REE from the water column during their descent to the sea floor. However, the long residence time of foraminifera at the sediment-water interface (of the order of hundreds of years) compared to their rapid fall through the water column (of the order of days [28]) strongly suggests that the major source of REE in the coating phase is either from bottom water or pore water. If inorganic scavenging of reactive dissolved elements (like the REE [8]) is an equilibrium process, with chemical exchange between trace elements associated with solid phases and the surrounding water [29,30], then during the long residence time of the foraminifera tests in the top 1 cm of the sediment the REE in the coating phase will have reached equilibrium with the REE in the pore waters and/or bottom waters.

Although there are, as yet, no published profiles of REE concentrations in pore waters, preliminary data (H. Elderfield, personal communication) suggest that there is a benthic flux of REE to the deep oceans. This tentative conclusion is supported by observations of near bottom enrichments of REE in the water column [9,11] and diagenetic recycling of REE in sediment underlying Mn nodules in areas of the Pacific Ocean [23].

Hence it is likely that REE in the coating phase are derived from interstitial waters, although scavenging of REE from bottom waters by Fe-rich flocs and subsequent inclusion in the coating phase cannot be ruled out, especially in light of the negative curvature observed for dissolved REE plots against conservative tracers in areas of the deep Atlantic [8,9,11].

The average REE concentrations in the coating phase are higher than generally reported for other FeMn-rich deposits (see Table 5). The lower concentrations observed in FeMn-rich deposits may be due to dilution of a REE-bearing Fe phase with diagenetic Mn [31] and uncertainties in determin-

ing the coating weight in this study.

To accurately assess the controls over the incorporation of REE in the coating phase we must have some knowledge of the distribution of dissolved REE in pore waters and bottom waters. As mentioned above, as yet there are no reliable measurements of REE concentrations in pore waters. There are some data available for bottom water REE concentrations in the Atlantic [9,11], and if, as seems likely, there is a REE benthic flux these waters will have a similar REE pattern to that of the uppermost pore waters in contact with the foraminifera at the sediment-water interface. However, the complex circulation of the deep Atlantic makes it difficult to distinguish between water mass effects and effects arising from aspects of the marine geochemical cycle of the REE. Whilst these problems are recognised it will be shown that the distribution of REE in the coating phase (relative to bottom waters) is consistent with their chemical properties and scavenging processes operating in the marine environment.

Fig. 4 illustrates the REE patterns of the coating phase and of bottom waters from the eastern equatorial Atlantic [11]. (The data of DeBaar et al. [9] were not used as these authors measured a different suite of REE, however their results are consistent with those data used here and would produce a similar pattern.) Also contained in Fig. 4 is the REE pattern obtained from normalising the coating REE concentrations to those in the bottom water. This latter REE pattern contains two distinct features. Part I shows a steep fall in the coating/water ratio from Eu to Yb, with part II showing a shallower rise from La to Eu.

The mechanism by which scavenging of trace metals by particulates takes place is complicated and not well understood. Explanations based on surface chemical theory [32] have not been entirely successful [29]. These studies are handicapped by the large number of particulate phases involved in the scavenging process [33]. A further complication is introduced by the detection of an organic film of unknown thickness on particulate surfaces which may have some impact on the scavenging process [34,35]. Balistrieri et al. [33] considered that pure oxides alone cannot account for the scavenging ability of sinking particulate matter.

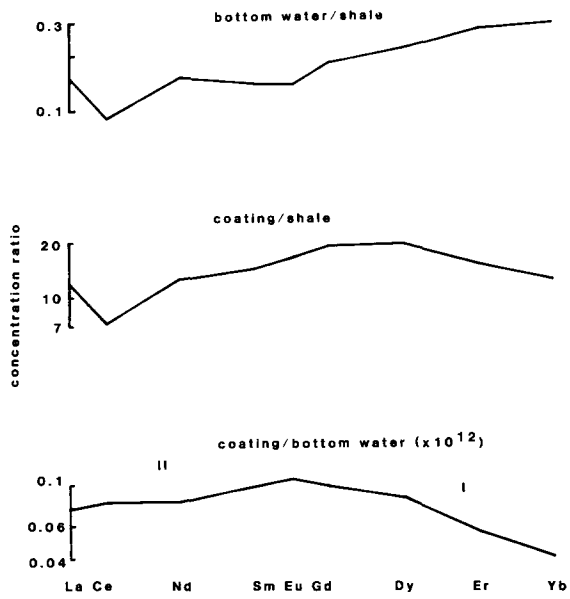

Fig. 4. Comparison between the REE patterns of Atlantic bottom water and in the coating phase.

They indicate that metal interactions with particulates are controlled by organic compounds coating the oxides or by organic compounds themselves. These organic-soluble metal interactions can be described by a reaction between organic carboxylic acid groups with the metal free ion. If this hypothesis is correct, the proportions of the dissolved REE present as the free ion will be important. The calculated speciations of the dissolved 3+ cations of the REE are illustrated in Fig. 5a [36]. The REE between Gd and Yb have distinctly lower percentages of the dissolved species present as the free ion relative to the lighter REE. This difference can be invoked to explain the enrichment of Eu over Yb in part II of the coating/water REE pattern. However, if this process was the sole control over the incorporation of REE in the coating phase, the relative free ion concentrations of Eu and La indicate that an enrichment of La over Eu should be observed in the coating water REE pattern; evidently this is not so.

Brewer and Hao [29] have shown that for some elements there is good agreement between the intensity of adsorption of trace metals onto par-

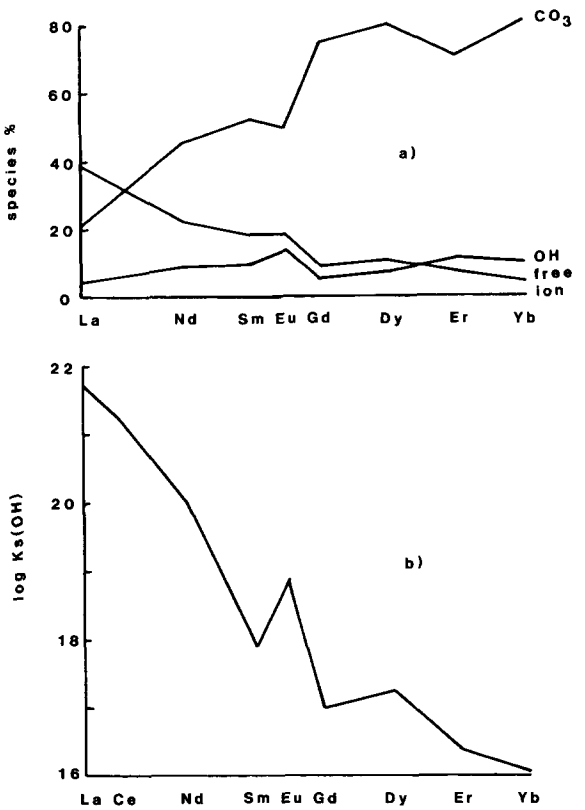

Fig. 5. (a) Calculated seawater speciations of the dissolved REE (from Turner et al. [36]). (b) Solubility products of the REE hydroxides [37].

ticulate matter and the stability of cation-hydroxide groups. The solubility constants (log K_s(OH)) for the REE hydroxides [37,38] are illustrated in Fig. 5b. There is a large decrease in solubility of the REE hydroxides on moving across the group from La to Gd, with less variability between the solubilities of the heavy REE hydroxides (the position of Eu may be anomalous as some authors [39] consider that the solubility of $Eu(OH)_3$ is similar to that of $Gd(OH)_3$). If it is assumed that the coating phase consists predominantly of Fe-oxyhydroxides [20] this variation in hydroxide solubilities can qualitatively explain the observed enrichments of Eu over La in part II of the coating/water REE pattern.

The general enrichment of the light REE over the heavy REE in the coating, and the strong enrichment of Eu over Yb, indicates that the relative free ion concentrations of the dissolved REE is a dominant control over the distribution of the REE between the coating and dissolved phases. This is in accordance with observations that for elements with similar surface stability constants (as would be expected for a chemically coherent group like the REE) the scavenging residence time is inversely related to the proportion of the dissolved metal present as the free ion [33,38]. However, the relatively high solubility of the light REE hydroxides, compared to those of the heavy REE, prevents their large enrichments in the coating phase predicted from free ion considerations alone, and leads to their depletion relative to Eu.

5.2 Lattice REE

The lattice phase REE concentrations are approximately an order of magnitude lower than the concentrations of REE in the non-detrital phase, and three orders of magnitude lower than the coating phase REE concentrations (see Table 5).

Shaw and Wasserburg [41] reported very low (20 nmol/g) concentrations of Nd in mollusc high-Mg calcite/aragonite but insufficient details were provided in this abstract to warrant a detailed comparison with the data from this study.

Oxygen isotope data indicate that the average calcification depth of Atlantic planktonic foraminifera is approximately 100 m [42]. The REE pattern obtained from normalising the average REE concentrations in 100 m deep Atlantic Ocean water [8,11] is illustrated in Fig. 6. Three values are given for Ce [8,9,11] to illustrate the greater variability shown by dissolved Ce concentrations in near surface waters relative to the other REE.

An alternative method of representing the enrichment of lattice REE relative to seawater dissolved REE is to use the distribution coefficient, K_D, where:

$$K_D = \left(\frac{(REE/Ca)_{lattice}}{(REE/Ca)_{seawater}} \right)$$

these values are presented in Table 6.

The mechanisms by which trace metals are included in the calcite matrix of foraminifera are complicated [43]. In addition to the chemical properties of calcite and the dissolved metals it is likely

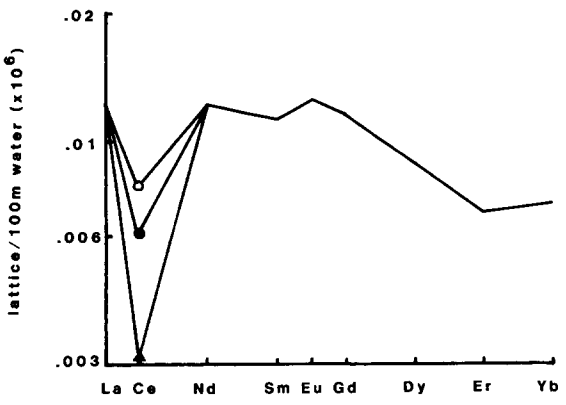

Fig. 6. Average lattice phase REE concentrations normalised to dissolved REE concentrations in 100 m Atlantic Ocean water. Except for Ce the REE concentrations are the average of data from Palmer [11] and Elderfield and Greaves [8]. The Ce concentrations are taken from Elderfield and Greaves [8] (open circle), Palmer [11] (closed circle) and DeBaar et al. [9] (triangle), see text for details.

that there are also biological ("vital") processes controlling the uptake of trace metals by plankton. Although the REE have not been shown to be required by organisms for their healthy metabolism it is known that other trace metals (e.g. Fe, Mn, Zn, Cu) are actively involved in planktonic biochemical processes [44]. It is not known whether plankton remove these, or other elements, from seawater as free ions or in the form of organic or inorganic complexes.

Several studies have shown that the ionic radii of the REE cations exert a major control over their substitution for Ca in a variety of mineral phases [45–47]. Fig. 7 illustrates the plot of K_D against REE ionic radii. The ionic radii are for the six coordinate ions (i.e., characteristic of substitution into the calcite structure) [48–50]. Note that both naturally occurring oxidation states of cerium (Ce^{3+} and Ce^{4+}) and europium (Eu^{2+} and Eu^{3+}) are considered; all other REE are considered to exist as 3 + cations in seawater.

There is a good correlation between K_D and the similarity of the ionic radii of the REE to that of Ca^{2+} The observation that both Ce^{4+} and Eu^{3+} lie on the trend line in Fig. 7 (whereas Ce^{3+} and Eu^{2+} do not) indicates the form in which they are removed from seawater [40]. Morgan and Wandless [46] have also noted that the light REE, with ionic radii similar to that of Ca^{2+}, are preferentially enriched in anhydrite relative to the smaller heavy REE cations.

Another factor which may influence the relative enrichment of the REE in foraminiferal calcite is the solubility of their carbonate salts. The distribution coefficients of the REE are substantially higher (130–170) than that of Cd (1.5) [3,51] despite the fact that both Ca^{2+} and Cd^{2+} form divalent cations and have similar ionic radii (1.00 Å and 0.95 Å respectively [47–49]). There are several possible

TABLE 6

Distribution coefficients for REE in foraminiferal calcite

Element	Lattice concentration (μmol/mol Ca)	Water concentration at 100 m (pmol/kg)	Distribution coefficient (K_D)
La	0.1854	15.3	125
Ce	0.1332	19.2	71
Nd	0.1624	13.3	126
Sm	0.0301	2.65	117
Eu	0.0074	0.59	130
Gd	0.0361	3.10	119
Dy	0.0337	4.10	84
Er	0.0243	3.57	70
Yb	0.0230	3.26	73

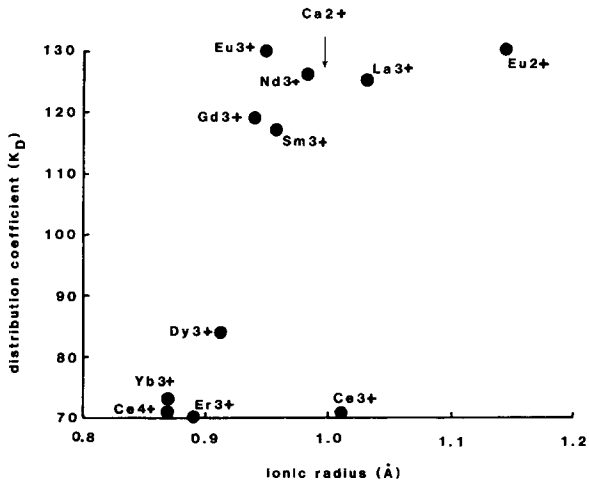

Fig. 7. Relationship between the distribution coefficient (K_D) and the ionic radii of the REE (ionic radii from Shannon and Prewitt [48–50]).

reasons for this apparent discrepancy. Although it is possible that vital effects result in foraminifera actively excluding Cd because of its toxicity, inorganic $CaCO_3$ precipitation experiments [52] also show Cd has a low distribution coefficient (13–30). The inorganic chemical properties of Cd and the REE also play important roles in determining their relative enrichments in foraminiferal calcite. An insight into the differences between the distribution coefficients of Cd and the REE can be obtained through solid-solution theory. The theoretical distribution coefficient is given by [32]:

$$K_{D\,ss} = \left(\frac{(K_s(CaCO_3))^3}{K_s\ Ln_2(CO_3)_3} \right)$$

where K_s is the solubility of the relevant carbonate salt. The distribution coefficients predicted from this equation are given in Table 7. Care must be taken in interpreting these numbers. A large source of uncertainty results from the experimental determinations of the solubility products which were not determined under standard or even equivalent conditions [53,54]. The observed distribution coefficients are lower than those predicted by the solubility products because of the increased activity coefficients of trace elements in a solid solute [32]. Although the limitations of the theoretical distribution coefficients must be recognised they are compatible with the observed K_D values. They correctly predict the general enrichment of the light REE in the calcite lattice relative to the heavy REE (see Fig. 8) and they predict the low K_D values for Cd compared to the REE. In addition, Turner and Whitfield [38] interpret the high concentrations of REE in many marine phases in terms of their high polarising power which results in stabilisation of the surrounding crystal structure.

TABLE 7

Comparison between calculated and observed calcite/seawater distribution coefficients for Cd and REE

Element	log K_s $MeCO_3$	log $K_{D\,ss}$	log $K_{D\,obs}$	Polarising power (z^2/r)
La	−26.4	8.1	2.1	8.7
Nd	−26.0	7.7	2.1	9.2
Sm	−25.5	7.2	2.1	9.4
Gd	−25.2	6.9	2.1	9.6
Dy	−24.5	6.2	1.9	9.9
Yb	−24.1	5.8	1.9	10.3
Cd	−11.7	5.6	0.2	4.2
Ca	−6.1	0	0	4.0

Solubility data are from Smith and Martell [48], corrected for seawater activity coefficients ionic strength following the Debye-Huckel theory [30,36].

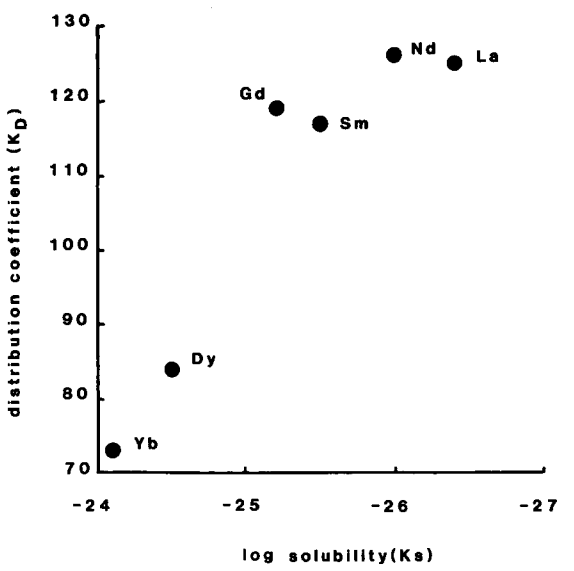

Fig. 8. Relationship between the distribution coefficient (K_D) and the solubility product of the REE carbonates ($K_s(CO_3)$). The solubility data are from Smith and Martell [53], corrected for seawater activity coefficients and ionic strength following the Debye-Huckel theory [30,36].

It was demonstrated above that the enrichment of the light REE relative to the heavy REE in the coating phase appears to be dependent, to some extent, on the proportions of the dissolved REE present as the free ion. Although the light REE have higher K_D values in the lattice and they have a higher proportion of free ions in the dissolved state, the relationship is not as clear as for the coating phase. This might be expected from the speculation that plankton do not take up trace metals as free ions, but probably as singly charged hydroxy or chloro complexes [44] and the even greater uncertainty regarding the relationship between the ion uptake and calcification processes.

TABLE 8

Evaluation of foraminifera as a REE carrier phase in the water column

Element	ΔREE/ΔCa in water column (mol ratio × 10^6)	REE/Ca in foraminiferal calcite (mol ratio × 10^6)
La	0.82	0.19
Ce	0.63	0.13
Nd	0.73	0.16
Sm	0.12	0.03
Eu	0.03	0.01
Gd	0.14	0.04
Dy	0.15	0.03
Er	0.13	0.02
Yb	0.13	0.02

5.3. The role of foraminifera in the marine geochemical cycle of the REE

If the lattice REE concentrations are compared to the REE/Ca ratios in the Atlantic water column [8,9,11] (see Table 8) it can be seen that foraminiferal calcite is not a significant carrier phase for REE in the oceans. However, if the data from this study are extrapolated on a global basis, the non-detrital phase (i.e., coating plus lattice) of calcareous sediments is a significant sink for the REE, removing 30% (for Ce) to 45% (for La) of the dissolved REE supplied to the oceans by riverine transport [55].

6. Conclusions

It has been demonstrated that the reductive cleaning techniques developed by Boyle [3] are successful in allowing the lattice REE concentrations of foraminiferal calcite to be precisely measured. This has also allowed the determination of REE concentrations in the FeMn-rich phase.

The REE distribution in the coating phase, relative to bottom water, is controlled by the proportions of dissolved REE present as the free ion, leading to a general enrichment of the light REE over the heavy REE, and by the relative stability of the REE-hydroxyl complexes, leading to a slight enrichment of Eu over La.

The distribution of the REE in the lattice phase, relative to REE seawater concentrations at the foraminiferal calcification depth, appears to be controlled by the similarity of the ionic radii of the REE cations to that of Ca^{2+} and by the solubility of the REE carbonate salts.

The consistency of the data presented here with the chemical properties of the REE paves the way for more detailed studies to explore the use of the lattice REE distributions as indices of palaeoceanographic conditions.

Acknowledgements

I am grateful to friends and colleagues at Cambridge and Leeds for their help and advice. I am particularly indebted to H. Elderfield (Cambridge) for his encouragement and assistance throughout this project and to E.A. Boyle (M.I.T.) who generously donated a sample for a comparative study and made several helpful suggestions that improved this manuscript. I also thank two anonymous reviewers for their thoughtful comments. Lamont-Doherty Geological Observatory core collection was supported by grants OCE 78-25448 (NSF) and N00014-80-C-0098 (ONR). Woods Hole Oceanographic Institute core collection was supported by grants OCE 81-25231 (NSF) and N00014-74-C-0262 (ONR). I acknowledge the support of NERC studentship GT4/80/GS/45 and support via NERC grant GR3/4444 to H. Elderfield.

Appendix 1—Core locations

Sample No.	Core	Location (lat., long.)
1	994 OK (0–10 cm)	34.2°S, 10.0°E
2	KNR54-6-100 27BC	63.0°N, 14.2°W
3	V23-41TW	62.0°N, 28.1°W
4	RC12-292TW	39.7°C, 15.5°W
5	CHN115-5-84 43PG	31.7°S, 20.9°W
6	V26-69TW	30.6°S, 15.7°W
7	V30-182	52.4°N, 30.4°W
8	RC16-77TW	12.7°S, 13.4°W
9	CHN82-6-26 26PG	42.2°N, 31.6°W
10	V30-96TW	39.9°N, 33.1°W
11	KNR31-3-1 1GPC	36.4°N, 32.0°W
12	CHN96-4-8 8PG	30.5°N, 20.3°W
13	AII92-2-27 7PG	22.9°N, 43.5°W
14	CHN75-2-29 19PG	12.9°N, 44.6°W
15	CHN99-3-15 12PC	4.6°S, 19.1°W
16	KNR54-6-94 24BC	59.4°N, 13.1°W
17	V22-31TW	1.9°N, 32.5°W
18	V29-180TW	52.7°N, 15.2°W
19	V24-260TW	12.4°N, 57.5°W
20	CHN41-1-2 2PC	17.3°N, 72.2°W
21	V26-22TW	26.3°N, 40.9°W
22	KNR31-5-13 13KC	28.6°N, 75.4°W
23	CHN96-4-1 1PC	27.4°N, 22.0°W
24	V29-153TW	1.0°N, 0.2°E
25	KNR-31-3-6 6GPC	33.9°N, 57.4°W
26	V22-180TW	3.3°S, 16.4°W
27	CHN47-1-34 3FF	30.5°N, 66.9°W
28	CHN115-5-58 37PG	37.0°S, 13.6°E
29	V30-91TW	36.4°N, 41.8°W
30	V9-31TW	8.2°N, 37.8°W
31	CHN99-3-34 25PG	8.7°S, 1.9°W

References

1 R.M. Cline and J.D. Hays, Investigation of late Quaternary paleoceanography and paleoclimatology, Geol. Soc. Am. Mem. 145, 1976.

2 N.J. Shackleton and J.P. Kennett, Paleotemperature history of the Cenozoic and the initiation of Antarctic glaciation: oxygen and carbon isotope analysis; DSDP sites 277, 279 and 281, in: J.P. Kennett, R.E. Houtz et al., Initial Reports of the Deep Sea Drilling Project, Vol. 29, pp. 743–755, U.S. Government Printing Office, Washington D.C., 1975.

3 E.A. Boyle, Cadmium, zinc, copper and barium in foraminifera tests, Earth Planet. Sci. Lett. 53, 11–35, 1981.

4 E.A. Boyle and L.D. Keigwin, Deep circulation of the North Atlantic over the last 200,000 years: geochemical evidence, Science 218, 784–787, 1982.

5 M.L. Delaney, Foraminiferal trace elements: uptake, diagenesis and 100 M.y. paleochemical history, Ph.D. Thesis, M.I.T., 1983.

6 D.Z. Piper, Rare earth elements in ferromanganese nodules and other marine phases, Geochim. Cosmochim. Acta 38, 1007–1022, 1974.

7 D.Z. Piper, Rare earth elements in the sedimentary cycle: a summary, Chem. Geol. 14, 285–304, 1974.

8 H. Elderfield and M.J. Greaves, The rare earth elements in seawater, Nature 296, 214–219, 1982.

9 H.J.W. DeBaar, M.P. Bacon and P.G. Brewer, Rare earth distributions with a positive Ce anomaly in the western North Atlantic Ocean, Nature 301, 324–327, 1983.

10 G.P. Klinkhamer, H. Elderfield and A. Hudson, Rare earth elements in seawater near hydrothermal vents, Nature 305, 185–188, 1983.

11 M.R. Palmer, Rare earth elements and Nd and Sr isotopes in the Atlantic Ocean, Ph.D. Thesis, University of Leeds, 1984.

12 W. Berger, J.S. Killingley and E. Vincent, Stable isotopes in deepsea carbonates: box core ERDC-92, west equatorial Pacific, Oceanol. Acta 1, 203–216, 1978.

13 A.W. Be and D.B. Ericson, Aspects of calcification in planktonic foraminifera, Ann. N.Y. Acad. Sci. 109, 65–81, 1963.

14 A. Hecht and S.M. Savin, Phenotypic variation and oxygen isotopes in recent planktonic foraminifera, J. Foram. Res. 2, 65–67, 1972.

15 R.B. Lorens, D.F. Williams and M.L. Bender, The early non-structural diagenesis of foraminiferal calcite, J. Sediment. Petrol. 47, 1602–1609, 1977.

16 M.L. Bender, R.B. Lorens and D.F. Williams, Sodium, magnesium and strontium in the tests of planktonic foraminifera, Micropaleontology 21, 448–459, 1975.

17 M.F. Thirlwell, A triple filament method for rapid and precise analysis of rare earth elements by isotope dilution, Chem. Geol. 35, 155–166, 1982.

18 S. Tsunogai, M. Nishimura and S. Nakaya, Complexometric titration of calcium in the presence of larger amounts of Mg, Talanta 15, 385–390, 1968.

19 M.A. Haskin and L.A. Haskin, Rare earths in European shales: a redetermination, Science 154, 507–509, 1966.

20 K.K. Turekian, A. Katz and L. Chan, Trace element trapping in pteropod tests, Limnol. Oceanogr. 18, 240–249, 1973.

21 M.L. Delaney and E.A. Boyle, Uranium and thorium isotope concentrations in foraminiferal calcite, Earth Planet. Sci. Lett. 62, 258–262, 1983.

22 K.B. Krauskopf, Introduction to Geochemistry, 615 pp., McGraw-Hill, New York, N.Y., 1979.

23 H. Elderfield, C.J. Hawkesworth, M.J. Greaves and S.E. Calvert, Rare earth element geochemistry of oceanic ferromanganese nodules and associated sediments, Geochim. Cosmochim. Acta 45, 513–528, 1981.

24 G. Arrhenius, M.N. Bramlette and E. Picciotto, Localization of radioactive and stable heavy nuclides in ocean sediments, Nature 180, 85–86, 1957.

25 J. Wright, R.S. Seymour and H.F. Shaw, REE and Nd isotopes in conodont apatite: variations with geological age and depositional environment in: Conodant Biofacies and Provinciales, D.L. Clark, ed., 1984.

26 S.K. Addy, Rare earth element patterns in manganese nodules and micronodules from the Nort West Atlantic, Geochim. Cosmochim. Acta 43, 1105–1115, 1979.

27 H. Elderfield and M.J. Greaves, Negative Ce anomalies in the rare earth element patterns of oceanic ferromanganese nodules, Earth Planet. Sci. Lett. 55, 163–170, 1981.

28 W.M. Sackett, Suspended matter in seawater, in: Chemical Oceanography, Vol. 7, 508 pp., Academic Press, London, 1978.

29 P.G. Brewer and W.M. Hao, Oceanic elemental scavenging, in: Chemical Modelling in Aqueous Systems—Speciation, Sorption, Stability and Kinetics, E.A. Jenne, ed., Am. Chem. Soc. Symp. Ser. 93, 261–274, 1979.

30 M.P. Bacon and R.F. Anderson, Distribution of thorium isotopes between dissolved and particulate forms in the deep sea, J. Geophys. Res. 87, 2045–2056, 1982.

31 S.E. Calvert, N.B. Price, G.R. Heath and T.C. Moore, Relationships between ferromanganese nodule composition and sedimentation in a small area of the equatorial Pacific, J. Mar. Res. 36, 161–183, 1978.

32 W. Stumm and J.J. Morgan, Aquatic Chemistry, 583 pp., Wiley, New York, N.Y., 1970.

33 L. Balistrieri, P.G. Brewer and J.W. Murray, Scavenging residence time of trace metals and surface chemistry of sinking particles in the deep ocean, Deep Sea Res. 28A, 101–121, 1981.

34 R. Neihoff and G. Loeb, Dissolved organic matter in seawater and the electric charge of immersed surfaces, J. Mar. Res. 32, 5–12, 1974.

35 K.A. Hunter and P.S. Liss, The surface charge of suspended particles in estuarine and coastal waters, Nature 282, 823–825, 1979.

36 D.R. Turner, M. Whitfield and A.G. Dickinson, The equilibration speciation of dissolved components in freshwater and seawater at 25°C and 1 atm. pressure, Geochim. Cosmochim. Acta 45, 855–881, 1981.

37 C.F. Baes and R.E. Messmer, The Hydrolysis of Cations, John Wiley, New York, N.Y., 1976.

38 D.R. Turner and M. Whitfield, Control of seawater composition, Nature 281, 468–469, 1979.

39 T. Moeller and N. Fogel, Observations on the rare earths, LXI. Precipitation of hydrous oxides from perchlorate solution, J. Am. Chem. Soc. 73, 4481, 1951.

40 E.D. Goldberg, Chemistry in the oceans, in: M. Sears, Oceanography, Am. Assoc. Adv. Sci. Publ. 67, 583–597, 1961.

41 H.F. Shaw and G.J. Wasserburg, Sm, Nd in modern and ancient marine $CaCO_3$ and apatite, Trans. Am. Geophys. Union 64, 335, 1983.

42 S.M. Savin and R.G. Douglas, Stable isotopes and magnesium geochemistry of Recent planktonic foraminifera from the Sourth Pacific, Geol. Soc. Am. Bull. 84, 2327–2342, 1973.

43 B.U. Haq and A. Boersma, Introduction to Marine Micropalaeontology, 322 pp., Elsevier, New York, N.Y., 1978.

44 D.H. Strickland, Production of organic matter in the primary stages of the marine food chain, in: Chemical Oceanography, Vol. 1, J.P. Riley and G. Skirrow, eds., 712 pp., Academic Press, London, 1965.

45 Y. Matsui, N. Onuma, H. Nagasawa, H. Higuchi and S. Banno, Crystal structure control in trace element partitioning between crystal and magma, Bull. Soc. Fr. Mineral. Crystallogr. 100, 315–324, 1977.

46 J.W. Morgan and G.A. Wandless, Rare earth element distribution in some hydrothermal minerals: evidence for crystallographic control. Geochim. Cosmochim. Acta 44, 973–980, 1980.

47 C.K. Brooks, P. Henderson and J.G. Ronsbo, Rare earth partitioning between allanite and glass in the obsidian of Sandy Braes, Northern Ireland, Mineral. Mag. 44, 157–160, 1981.

48 R.D. Shannon and C.T. Prewitt, Effective ionic radii in oxides and fluorides, Acta Crystallogr. B25, 925–946, 1969.

49 R.D. Shannon and C.T. Prewitt, Revised values of effective ionic radii, Acta Crystallogr. B26, 1046–1048, 1970.

50 R.D. Shannon, Revised effective ionic radii and systematic studies of interatomic distances in halides and chalcogenides, Acta Crystallogr. A32, 751–767, 1976.

51 E.A. Boyle, F.F. Sclater and J.M. Edmond, On the marine geochemistry of cadmium, Nature 263, 42–43, 1976.

52 R.B. Lorens, Sr, Cd, Mn and Co distribution coefficients in calcite as a function of calcite precipitation rate, Geochim. Cosmochim. Acta 45, 553–561, 1981.

53 R.M. Smith and A.E. Martell, Critical Stability Constants, Vol. 4, Plenum Press, New York, N.Y., 1976.

54 N. Jordanov and I. Havezov, Loslichkeitsprodukte der normalen Carbonate einiger dreiwertiger Seltner Erden ($E_2(CO_3)_3 \cdot nH_2O$), Z. Anorg. Allg. Chem. 347, 101–106, 1966.

55 J. Hoyle, H. Elderfield, A. Gledhill and M.J. Greaves, The behaviour of the rare earth elements during mixing of river and seawaters, Geochim. Cosmochim. Acta 48, 143–149, 1984.